Accepted Manuscript

Fragment-Based Design, Synthesis, Biological Evaluation, and SAR of 1*H*-benzo[*d*]imidazol-2-yl)-1*H*-indazol Derivatives as Potent PDK1 Inhibitors

Ting Chen, Venkataswamy Sorna, Susie Choi, Lee Call, Jared Bearss, Kent Carpenter, Steven L. Warner, Sunil Sharma, David J. Bearss, Hariprasad Vankayalapati

PII: S0960-894X(17)31035-1
DOI: https://doi.org/10.1016/j.bmcl.2017.10.041
Reference: BMCL 25370

To appear in: *Bioorganic & Medicinal Chemistry Letters*

Received Date: 13 August 2017
Revised Date: 3 October 2017
Accepted Date: 19 October 2017

Please cite this article as: Chen, T., Sorna, V., Choi, S., Call, L., Bearss, J., Carpenter, K., Warner, S.L., Sharma, S., Bearss, D.J., Vankayalapati, H., Fragment-Based Design, Synthesis, Biological Evaluation, and SAR of 1*H*-benzo[*d*]imidazol-2-yl)-1*H*-indazol Derivatives as Potent PDK1 Inhibitors, *Bioorganic & Medicinal Chemistry Letters* (2017), doi: https://doi.org/10.1016/j.bmcl.2017.10.041

Bioorganic & Medicinal Chemistry Letters
journal homepage: www.elsevier.com

Fragment-Based Design, Synthesis, Biological Evaluation, and SAR of 1*H*-benzo[*d*]imidazol-2-yl)-1*H*-indazol Derivatives as Potent PDK1 Inhibitors

Ting Chen[a], Venkataswamy Sorna[c], Susie Choi[c], Lee Call[c], Jared Bearss[b], Kent Carpenter[b], Steven L. Warner[b], Sunil Sharma[c], David J. Bearss[b *], Hariprasad Vankayalapati[c *]

[a] *Department of Physiology & Developmental Biology, Brigham Young University, Provo, UT 84602 U.S.A.*
[b] *Tolero Pharmaceuticals, Inc., 2975 Executive Parkway, Suite 320, Lehi, UT 84043, U.S.A.*
[c] *Division of Oncology of School of Medicine and Center for Investigational Therapeutics at Huntsman Cancer Institute, University of Utah, 2000 Circle of Hope, Salt Lake City, UT 84112 U.S.A.*

ARTICLE INFO

Article history:
Received
Revised
Accepted
Available online

Keywords:
PDK1 inhibitor
Fragment-based design
1*H*-benzo[*d*]imidazol-2-yl)-1*H*-indazoles
AN3-CA
DUSP6
DUSP4
FOSL1
KATO-III
MV4-11

ABSTRACT

In this work, we describe the use of the rule of 3 fragment-based strategies from biochemical screening data of 1100 in-house, small, low molecular weight fragments. The sequential combination of *in silico* fragment hopping and fragment linking based on S160/Y161/A162 hinge residues hydrogen bonding interactions leads to the identification of novel 1*H*-benzo[*d*]imidazol-2-yl)-1*H*-indazol class of Phosphoinositide-Dependent Kinase-1 (PDK1) inhibitors. Consequent SAR and follow-up screening data led to the discovery of two potent PDK1 inhibitors: compound **32** and **35**, with an IC_{50} of 80 nM and 94 nM, respectively. Further biological evaluation showed that, at the low nanomolar concentration, the drug had potent ability to inhibit phosphorylation of AKT and p70S6, and selectively kill the cancer cells with mutations in both PTEN and PI3K. The microarray data showed that DUSP6, DUSP4, and FOSL1 were down-regulated in the sensitive cell lines with the compound treatment. The *in vivo* test showed that **35** can significantly inhibit tumor growth without influencing body weight growth. Our results suggest that these compounds, especially **35**, merit further pre-clinical evaluation.

* Corresponding author's e-mail: hari@hci.utah.edu, dbearss@toleropharma.com

The Phosphoinositide-Dependent Kinase-1 (PDK1), by passing the signal down to the AKT, plays the central role in PI3K/AKT/mTOR pathway. Several AGC super family kinases including PKC, SGK, PKB/AKT, p70S6K, and PDK1 itself can be phosphorylated by PDK1. Mutations in genes (PI3K and PTEN) that regulate PIP3 production exist in variety of tumors, such as breast, ovarian, prostate, gastric, lung, and hematological cancers. These mutations usually lead to elevated levels of PIP3, which can enhance the activation of PKB/AKT, p70S6K, and SGK. Inhibitors of PDK1 present a viable therapeutic option for the treatment of PDK1 elevated cancer types[1]. If the selective PDK1 inhibitor that was also orally bioavailable small molecules can be discovered, it would show the most desirable therapeutic effect in these cancers, particularly ovarian cancers where the physiological role of the PDK1 mediated pathway is well defined[2].

Fragment-based lead discovery has become a powerful tool for the discovery and optimization of potent leads[3,4]. As a substitute to more conventional high-throughput screening methods of hit identification process, the screening of low molecular weight (MW <300 Da) and less lipophilic (clog P < 3) fragments can often serve as key moieties for the identification of novel, tractable hits with a high hit rate[5]. These fragments exhibit superior ligand efficiency and can be improved into potent leads with promising "rule of five" properties. Thus, the design and optimization on the final lead compound performed by identifying and optimizing individual, high ligand efficient fragments. This is followed by the synthetic linkage of two or more fragments to produce the required affinity for the target protein with ideal lead-like properties. The main advantage of fragment-based design techniques is that it requires the synthesis and testing of fewer compounds and significantly increases the amount of chemical space tested by using a comparatively small library of compounds.

In the present study, structural analysis of a previously reported crystal structure of PDK1 kinase[6] bound to BX-320 facilitated the primary design and subsequent discovery of novel 1H-benzo[d]imidazol-2-yl)-1H-indazoles PDK1 inhibitors[7,8,9]. Two (**32** and **35** in Table 1) of the compounds we discovered showed low nanomolar activity in 10 dose-response curve cell viability assays, particularly in cell lines with PTEN and PI3K mutations[7]. When compound **32** screened against 21 kinases, it showed good potency against PDK1. Compound **32** also effectively lowered phospho-AKT (Thr308) levels in a dose-dependent manner.

Design and Synthesis of PDK1 Inhibitors: We employed fragment-based virtual screening, using varied selection of shape similarity methods for searching commercially available compound databases for molecules with similar configurations, but altered chemical connectivity when compared to the known PDK1 inhibitors BX-320, and BX-517[10]. Additionally, the application of fragment-based design strategies coupled with knowledge-based scaffold-hopping led to the collection of approximately 1100 low molecular weight fragments[11,12,13] that were physically acquired and screened in a luciferase-based PDK1 biochemical kinase assay[14]. The combination of in silico virtual screening based on hydrogen bonding to amino acid residues (Ser160/Ala162) in the hinge region of PDK1 and a biochemical kinase assay led to the identification of multiple PDK1 inhibitor scaffolds that were all within the "rule of three" criteria of chemical space, suggesting they were suitable for further optimization[15, 16].

Active fragments and their binding modes were validated using protein-ligand computational methods and the PDK1 crystal structure[6] (PDB ID: 1Z5M). IC_{50} values for the five most active fragments were between 29-122 μM of which 4-iodo-1H-indazol-3-amine (3) and 6-bromo-1H-indazol-3-amine (4) (Figure 1A and 1B) showed the most significant promise based on the results of the biochemical assay and information obtained from computational efforts.

Figure 1A. Both the panels depict the binding mode of fragment 3 within the PDK1 ATP binding site. The dashed line in blue/red shows hing hydrogen bonding interactions. Critical residues labeled and depicted in surface representation.

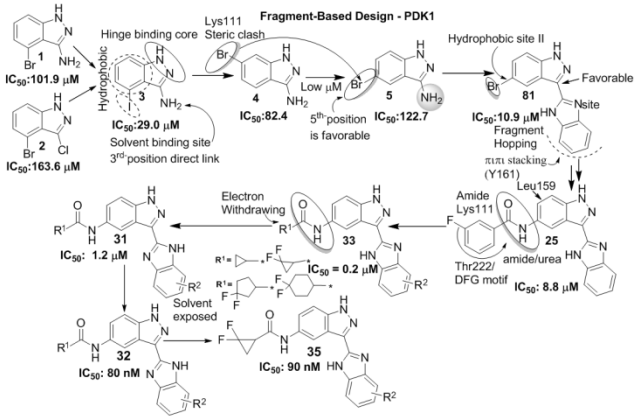

Figure 1B. Chemical structure of fragment hits 1-5 to leads and its PDK1 activities.

Compared to the other hits, these two fragments demonstrated sufficient potency and ligand efficiency that allowed for further optimization to more complex lead candidates possessing the required potency and selectivity toward PDK1. Furthermore, these

fragments appeared to be excellent starting points for optimizing cellular activity and the physicochemical properties required to investigate candidate compounds in pre-clinical studies and, ultimately, in clinical trials. The ICM and GOLD docking experimental results on these fragments provided a clear rational on the less potent activities of the 5- or 6-bromo-1H-indazol-3-amines (fragments **1** and **5**) based on its binding mode when compared to the corresponding, more potent activity of 4-iodo-1H-indazol-3-amine (**3**) fragment series. The 6th position of bromine atom in fragment **1** is involved in direct steric clash with Leu111 residue which is located in the hydrophobic site of PDK1. In the case of 5-Br-1H-indazol-3-amine fragment (**1**), 5-Br substitution positioned towards Thr122 residue of PDK1 pocket, whereas the indazole involved in interactions with Tyr122 is retained, albeit with weak binding energy compared to the active hit fragment 4-iodo-1H-indazol-3-amine (**3**). Utilizing 3-D crystal structures[6], computational screening, and standard medicinal chemistry efforts, fragments **3** and **4** systematically optimized to yield small molecule inhibitors (Figure 1B) with a significant improvement in potency toward PDK1 and possessing favorable physicochemical properties[15, 16] for drug development.

Several of the compounds demonstrated mid-nM inhibitory activities against PDK1 and several rounds of optimization afforded two compounds, namely compounds **32** and **35**. These lead compounds exhibited potent PDK1 activity with IC_{50} values of 80 and 90 nM, respectively (Table 1). The known PDK1 inhibitor BX-517 was used as positive control exhibited an IC_{50} of 9 nM. These compounds discovered through the exploration of SAR at the R^1 and R^2 positions of the core scaffold (Scheme 1). Initial studies were aimed at the substitutions of the directly attached 5-position of indazole ring (**19-21**, Table 1), which were prepared from commercially available phenylboronic acids. Evaluation of compounds **19-23** indicated that either 3-substituted methylsulfone (**19**), hydrophobic, electron withdrawing groups (**20**), or a cyclopentylurea (**23**) show poor PDK1 kinase inhibitory activity. However, the introduction of a 2-methyl-2-phenylpropanenitrile at the fourth position (**21**) showed a modest improvement in activity (IC_{50} = 5.2 µM) and provided a path for further optimization[17].

Table 1. Inhibition of PDK1 by 1*H*-benzo[*d*]imidazol-2-yl)-1*H*-indazol derivatives.

Compd	Structure	[a]IC_{50} µM	Compd	Structure	[a]IC_{50} µM
19		15.3	**20**	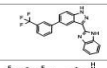	30.3
21	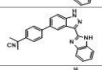	5.2	**22**	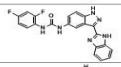	[b]NA
23	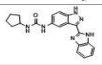	53.9	**24**	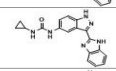	0.9
25	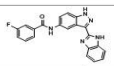	8.8	**26**	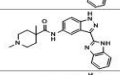	12.4
27	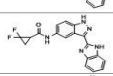	0.3	**28**	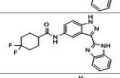	0.4
29	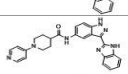	[b]NA	**30**	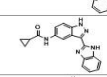	1.2
31		1.2	**32**	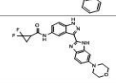	0.08
33	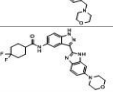	0.2	**33**	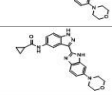	0.2
35	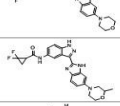	0.09	**36**	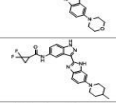	0.8
37		0.4	**38**	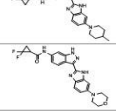	[b]NA

[a] Supporting information for assay details, [b]NA = Not Active

The introduction of an amide with a small cycloalkyl ring substituent, such as cyclopropyl (**30**, IC_{50} = 1.23 µM), or adding electron-withdrawing groups, such as fluorine atoms, was well tolerated and significantly improved the PDK1 activity to 280 and 410 nM (**27** and **28** respectively). Introduction of an amide substituted heteroaryl group, such as in compound **25**, was not tolerated. Extending morpholine amide moiety with greater flexible spacer and basic benzyl morpholine that is slightly basic moiety resulted in a significant loss of its activity, as seen with compound **31**. We further explored the effects of moving the amide position by making compound **37**, which exhibited only mildly potent activity against PDK1 (IC_{50} = 385 nM). Similarly, moving the substituent to the sixth position of the 1H-indazole ring completely abolished PDK1 activity (**38**). In comparison, the insertion of a 2, 2-difluoro cyclopropyl substituent and a directly substituted morpholin provided potent PDK1 inhibitory activity (**32**) with a IC_{50} value of 80 nM.

The predicted binding modes of these fragments and actual compounds we synthesized were confirmed by ICM[18] docking and molecular dynamic simulations within the active site of PDK1 kinase domain when in complex with compound 32 (Figure 1C). These results revealed that the 1*H*-indazoles of 1*H*-benzo[*d*]imidazol-2-yl)-1*H*-indazole scaffold and its -N atoms involved in a critical interaction with the hinge region of the PDK1 through a potential hydrogen bond with the backbone of Ser160. Besides that, another hydrogen bond forms between the backbone -N atom of Tyr161 and the second -N atom in the indazole scaffold of compound **32**. Whereas the benzo[*d*] imidazol ring involved in pi-pi stacking interactions with the aryl ring side chain of Tyr161. The fused aryl ring of the 1*H*-indazole associated with non-bonded interaction with side chains of the Leu159 residue located at the gate-keeper site, and had a favorable hydrophobic contact between aryl ring of 1*H*-indazole, side chain of Leu88 and the backbone atoms of Gly89. The 2, 2-difluoro-N-phenylcyclopropanecarboxamide group participates in multiple interactions with Glu90, Gly91 and Lys111 residues.

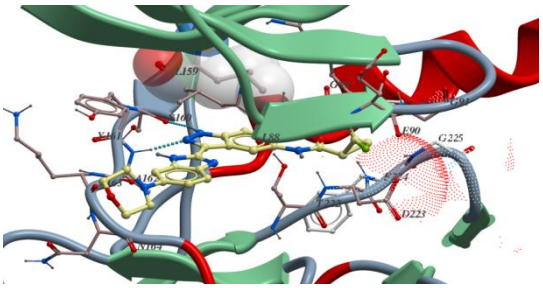

Figure 1C. Compound **32** in complex with PDK1. Docking model of the complex formed between compound **32** and the PDK1 crystal structure model (ID: 1Z5M) of the ATP binding site. The critical residues involved in H-bonding interaction shown solid dashed lines. The gatekeeper L159 and DFG sites depicted with CPK and dotted surfaces.

The amide carbonyl group oriented within hydrogen-bonding distance of Lys111. The 2, 2-difluorocyclopropyl rings occupy a hydrophobic portion of the cavity surrounded by the DFG loop and the side chain of Thr122. To explore the solvent binding site, several compounds with a morpholine ring substitution at the 6th position of 1*H*-benzo[*d*]imidazol improved the physicochemical properties of compounds and improved the cell-based activity as seen with compound **35** against AN3-CA cells. The morpholine group positioned at the solvent binding site is also involved in interactions with Lys165 (Figure 1C). The introduction of 2-methyl morpholine did not significantly alter the PDK1 kinase activity, whereas the introduction of a one-carbon spacer (**31**) abolished the PDK1 activity (1.22 mM). The addition of this flexible spacer caused a conformational shift of the molecules losing the hydrogen bond interactions with the hinge region. The *in vivo* pharmacokinetic profile of compound **32** is in evaluation, but based upon the *in vitro* profile, compound **32** and **35** represent attractive starting points for a more extensive medicinal chemistry program to optimize the molecules. The entire series of compounds synthesized during this optimization effort is shown in Table 1.

To synthesize 1*H*-benzo[*d*]imidazol-2-yl)-1*H*-indazoles series, we followed the synthesis outlined in Scheme 1, starting with the THP protected substituted aldehyde **7** and treated it with aryl-1,2-diamine in concentrated HCl and $NaHSO_3$, which provided the (1*H*-benzo[*d*]imidazol-2-yl)-1-(tetrahydro-2*H*-pyran-2-yl)-1H-indazole (**9**). In subsequent steps for the synthesis of compounds **19-21**, variously substituted aryl boronic acid groups were added under cross-coupling $Pd(OAc)_2$, PPh_3 conditions in presence of Na_2CO_3 in THF followed by subsequent deprotection in presence of TFA and DCM, which afforded compound **10** and **11**, respectively.

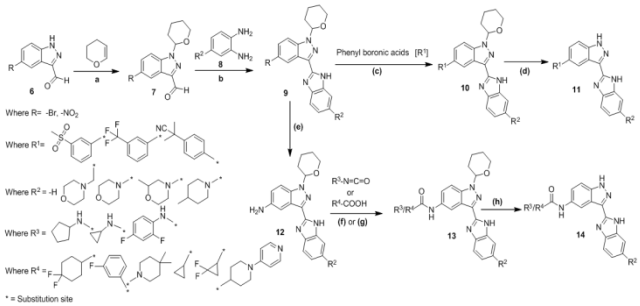

Scheme 1[a]**.** Synthesis of 1*H*-benzo[*d*]imidazol-2-yl)-1H-indazoles series. [a]Reagents and conditions: (a) TsOH (0.1 eq), THF:DCM (1:1), RT, 4-6h; (b) (i) con.HCl, THF, 65 ^oC, 30 min (ii) $NaHSO_3$, Reflux, 12h; (c) $Pd(OAc)_2$, PPh_3, Na_2CO_3, THF, Reflux, 12h; (d) TFA, DCM, RT, 12h; (e) 10% Pd/C, H2, Ethanol, RT; (f) Pyridine, DCM, RT; (g) HOBt, EDC, NaHCO3, DMF, RT, 24h; (h) TFA, DCM, RT,12h.

The R^2 substitutions were instituted using the substituted 1, 2-dinitrobenzene (**15**) as starting material provided in Scheme 2[18]. Additional analogues outlined in Table 1 were prepared from compound **9** by reduction under 10% Pd/C in EtOH in presence of H_2 leading to **12**. Compound **12** was subsequently transformed to urea or amide (**13**) using base or HOBt/EDC coupling conditions followed by a deprotection step leading to compound **14** (*see* Supporting Information for details) and variously substituted compounds **22-34** given in Table 1.

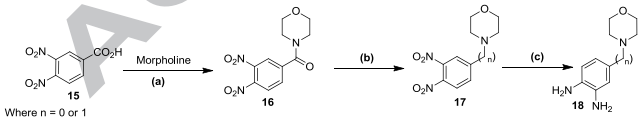

Scheme 2[b]**.** Synthesis intermediates. [b]Reagents and conditions: (a) $SOCl_2$, Et_3N, DMF, THF; (b) $NaBH_4$, $BF_3.OEt_2$, THF; (c) 10% Pd/C, H_2, Ethanol, RT.

To sum up, only compounds **32** and **35** can inhibit PDK1 at the low nanomolar concentration, so the following part will focus on these two compounds.

Kinase Selectivity Profiling: To explore kinase specificity toward PDK1, **32** was screened at a single concentration (500 nM) against a panel of relevant kinases for selectivity profiling (Figure. 2). In addition to PDK1, **32** showed appreciable activity against p70S6K, which is downstream of the PI3K/AKT pathway. Compound **32** also inhibited VEGFR1/2 and PDGFRA with reasonable potency. Therefore, not only the kinases in PI3K/AKT pathway, but also the ones in the MAPK pathway were inhibited by **32**. More efforts were still needed in order to make **32** a pure PDK1 inhibitor. The kinase selectivity profile of **35** has not been determined, although it is expected to be similar to **32**.

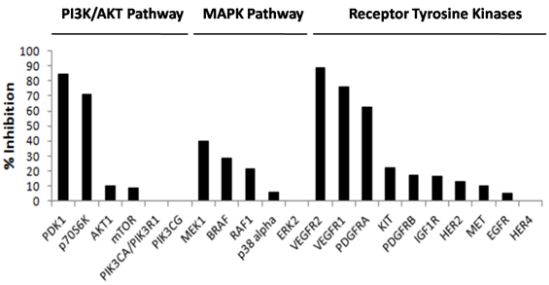

Figure 2. Kinase selectivity profile for compound **32**.

Cell-based Activity: To assess the activities of **32** in relevant cell-based assays, the compounds were screened in cell viability assays against three PI3K/AKT pathway mutation cancer cell lines: AN3-CA, RL-95-A, and HEC-1A (Figure 3).AN3-CA cells have mutations in both PTEN and PIK3R1 (regulatory subunit of PI3K). RL-95-A cells have mutations in PTEN and in H-RAS (can regulate PI3K). HEC-1A cells are mutated in PIK3CA (catalytic subunit of PI3K). Interestingly, **32** efficiently killed AN3-CA cells at the lower concentration with an IC_{50} of 39.0 nM, but the IC_{50} for RL-95-A and HEC-1A cell lines were at 449.1 nM and 3.4 μM. (Figure 3). The activity for **35** was similar to **32**. The IC_{50} for **35** treated AN3-CA cells was 0.02 μM, and for **35** treated RL-95-A was 0.7 μM. (Data not shown)

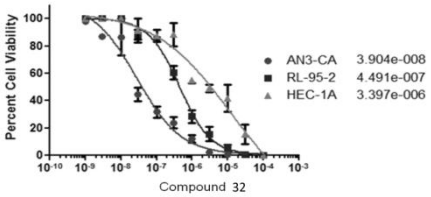

Figure 3. Inhibition of cell viability in the selected endometrial cancer cell lines (AN3-CA, RL95-2, and HEC-1A) using compound 32.

These preliminary results from a small panel of cell lines suggested that the cancer cell lines with PTEN and PI3K mutations, like AN3-CA cells, were more sensitive to **32** and **35**. It seems like that lost PTEN function and PI3K activation are important for the sensitivity to **32** and **35.** To confirm this importance, a special cell line, HS578T, that has mutated PIK3R1 and wild type PTEN was used. We knocked-down PTEN using shRNA and see if modified HS578T can be sensitive to **32** and **35**. A cell viability assay showed that loss of PTEN sensitized this cell line to both **32** and **35**, lowering the IC_{50} of **32** from 3.1 to 1.2 mM and that of **35** from 2.2 to 0.80 mM (Figure. 4).

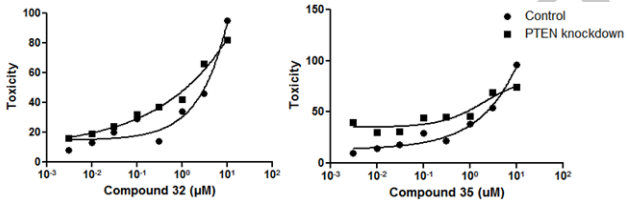

Figure 4. Toxicity of compound **32** and **35** on HS578T transduced with PTEN shRNA or control shRNA. Toxicity represents cell death percentage.

To further explore how PI3K/AKT/mTOR pathway was affected by **32** in AN3-CA cells. Phospho-AKT (Thr308) was checked using the Meso Scale Discovery technology platform after 24 hours treatment (Figure. 5A). **32** showed good ability of down-regulating pAKT (about 50%) with lower concentration (100nM). Furthermore, phosphorylation of ribosomal protein s6, the downstream of PI3K/AKT/mTOR pathway, were also checked using an in-cell western, (Figure. 5B). Both **32** and **35** showed great ability of decreasing phosphorylation of s6 with EC_{50} values of 75.6 nM and 76.7 nM, respectively.

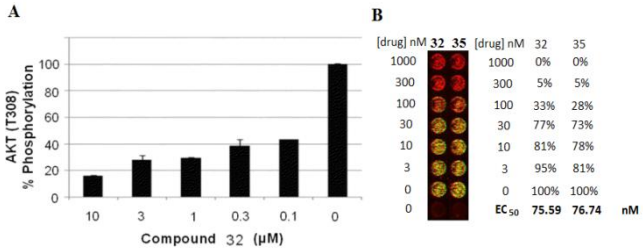

Figure 5. A. Phosphorylated AKT (T308) levels in AN3-CA treated with different concentrations of compound **32** for 24h. **B.** Visual overlay of total ribosomal protein s6 (red) and phospho-ribosomal protein s6 (green). Image appears yellow where both channels overlap. Quantification of signal intensity and EC_{50} values for the two drugs used shown on the right.

Cell-line screen: To find out more sensitive cell lines for **32** and **35**, a large cell line panel of over 100 cancer cell lines was screened with these two compounds. Both **32** and **35** demonstrated remarkable selectivity for cell killing in several cell lines (KATO3, KG-1, MV4-11, Kasumi-1, MFE296 and AN3-CA) in the low nanomolar range compared to all of the remaining cell lines in which the compounds showed low micromolar activity (Table 2 in supporting information). The cell lines that turned out to be highly sensitive had PTEN deletions or silencing as well as activation of PIK3CA through activating mutations in PIK3CA or RAS proteins.

Microarray check: Then we ran the whole genome microarray for the ten different cell lines (six primary sensitive cell lines: KATO3, KG-1, MV4-11, Kasumi-1, MFE296, AN3-CA; and four insensitive cell lines: J82, Molt4, HEC1A, MFE280) and each cell line treated with either **32**, **35**, or DMSO control. Single replicates of each treatment performed. RNA degradation plot (Figure 6a in supporting information) and the density plot (Figure 6b in supporting information) show no degradation of the samples and the density plots of all the arrays were quite similar. We tried applying linear models to the data, to find cell-line-specific and drug-specific effects, but it is impossible to identify any cell line/drug interaction effects. Then we attempted to simplify the patterns of expression displayed in Figure 6c (Supporting information) by applying k-means clustering across the expression profiles of the 5144 genes showing changes > 2-fold. This technique groups the expression profiles into k different clusters, and we hope the k is a small number, the variance within each of the k clusters is small, and the variance between the clusters is large. Even at values of k as large as 40, however, the variance within the clusters is quite high: 40% of the total. This implies that the expression profile landscape is very complex, due to many different patterns of expression across the cell lines. However, all hierarchical cluster results showed that the samples clustered primarily by cell line, that the response to either compound was relatively subtle compared to the differences between cell lines, and that the response to the two compounds was similar within each cell line, but was different between the cell lines. Therefore, we looked at the similarity of response to the two treatments within each cell line by generating scatter plots comparing **32**/DMSO expression and **35**/DMSO expression and calculated the Pearson's correlation between the **32**/DMSO and **35**/DMSO ratios for each cell line. We noticed that the correlation was highest among four of the sensitive cell lines (AN3-CA: 0.900, KATO3: 0.886, KG-1: 0.886, and MV4-11: 0.890), and that each of those cell lines showed a handful of genes with large decreases of expression (> 4-fold down) in both **32** and **35** treated cells (Figure 6d in supporting information). Figure 6d (Supporting information) shows that, although each cell line has its own group of highly down-regulated genes, the 4 cell lines share several genes that are highly down-regulated: DUSP6, FOSL1, and to a lesser degree DUSP4.

RT-PCR and Western: To further confirm the results from microarray analysis, 7 cell lines (3 sensitive cell lines, AN3-CA, KATO3, MV4-11 and 4 insensitive cell lines, HCT-116, CAPAN-1, SW480, Molt4) were treated with **35** at three different concentrations (1μM, 0.1μM and 0.01μM), and then checked the mRNA expression level for those three shared genes (DUSP6, FOSL1 and DUSP4). **35** can down-regulate the transcription of those 3 genes in the three sensitive cell lines, but the regulate directions are quite different in those four insensitive cell lines (Figure 7 in supporting information). Then, Western blot was done to confirm the change in the protein level, and the results showed the same changing direction (Figure 8). For the sensitive cell lines, the protein level for DUSP6, FOSL1 and DUSP4 all decreased with **35** treatment, while this is not true for the insensitive cell lines. PDK1 mRNA (Figure 7 in supporting information) and protein (Figure 8) expression level had also been checked, but didn't show any consistent change in either sensitive or insensitive cell lines.

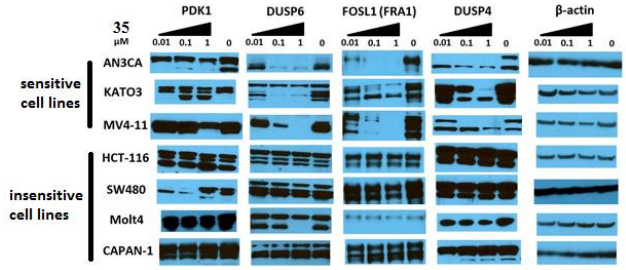

Figure 8. Western Blot for PDK1, DUSP6, FOSL1, DUSP4, and β-actin in three sensitive cell lines (AN3-CA, KATO-3 and MV4-11) and four insensitive cell lines (CAPAN-1, HCT-116, SW480 and Molt4) after **35** treatment.

ShRNA: To see if down-regulating DUSP6, FOSL1 or DUSP4 are the key factors that contribute to the **35**-induced sensitive cancer cell lines death; si-RNA (all purchased from Thermo Scientific) experiments had been done to the three sensitive cell lines. ShRNA had also been used to knockdown PDK1 to imitate the **35**'s PDK1 inhibitory effect. After transfection at the optimal condition, ATPLite assay has been used to reflect the amount of alive cells. The results showed that knocking-down DUSP6, FOSL1 or DUSP4 individually can kill the sensitive cell lines, but not as well as knocking-down PDK1 (Figure 9a in supporting information), while knocking-down PDK1 and 35 treatment shown the really similar killing effect (Figure 9b in supporting information). For MV4-11 cell line, just knocking-down DUSP6 shown the same effect as knocking down PDK1. For KATO3 cell line, knocking-down DUSP4 seems more important for killing the cell. For AN3-CA, the important role seems to switch to FOSL1.

***In vivo* Efficacy:** To demonstrate *in vivo* activity in a preliminary animal efficacy model, initially the study protocol was submitted for review and was approved by Huntsman Cancer Institute's IACUC.We did subcutaneous implantation to put AN3-CA cells into athymic nude mice at the hind flank. Then wait until the tumors reached a size of approximately 200 mm^3, mice were then stratified into three groups and intraperitoneally (IP) administered either vehicle, **32**, or **35**. The compounds were formulated in a solution of 20% DMSO, 20% cremophor, and 60% water and dosed at 50 mg/kg daily Monday through Friday for two weeks. Tumors and body weights were measured twice a week and are shown in Figure 10A and Figure 10B, respectively. Compound **32** caused only a minor decrease in tumor burden compared to the vehicle control that was not significant. However, treatment with **35** led to a significant decrease in tumor size; at the end of the two-week study, the group treated with **35** had on average tumors about one-third the size of the vehicle treated group. Furthermore, neither **32** nor **35** caused any body weight loss during the whole study. In fact, the animals continued to gain weight at a rate that was very similar to the animals in the vehicle group. These results suggest that both compounds, but particularly **35**, has *in vivo* efficacy at dose levels that are not toxic to the animals.

Phosho-s6 was also checked by western blot in the tumors from the vehicle and **35** groups (Figure 10C). Phospho-s6 level decreased in the **35** treated group, not vehicle group. Total-s6 level didn't change. These data suggest that **35** targets the PDK1/ p70S6K pathway and **35** decreases the p-S6 to inhibit tumor growth.

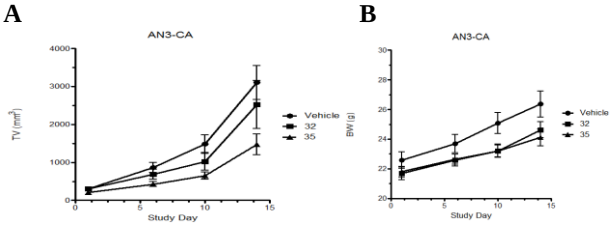

Figure 10 A and **B.** Tumor volumes (A) and body weights (B) of nude mice IP injected with compound **32**, **35**, or vehicle for two weeks.

Figure 10 C. Total and phosphorylated ribosomal protein s6 levels in tumor samples from mice treated with vehicle or compound **35**.

Discussion: Substantial preclinical and even clinical evidence now exists suggesting that targeting the PI3K/AKT pathway will have therapeutic benefit in some types of cancer. Numerous PI3K inhibitors and AKT inhibitors are at multiple stages of development, along with several mTOR inhibitors, some of which are now approved anti-cancer agents. Clearly, this pathway represents an exciting area for drug development and can, hopefully, provide patients and physicians with new options to treat various malignancies. PDK1 is a vital component to this signaling pathway that, in our view, has not been completely explored as a therapeutic target. PDK1 is required for full activation of AKT and is frequently constitutively activated due to loss of PTEN and mutations in PI3K. Early knockout animal studies suggest that PDK1 inhibition may overcome the consequences of these genetic alterations in cancer and this has been corroborated by more recent target validation studies using small molecules and shRNA approaches.

Using a fragment-based, structure-assisted approach[19, 20, 21], lead compounds **32** and **35** were discovered as fairly potent PDK1 inhibitors. When profiled against a small panel of kinases, **32** also demonstrated activity against p70S6K, which functions downstream of AKT and by itself, represents a potential therapeutic target. Even though **32** had some off-target effect (can strongly inhibit VEGFR1/2 and PDGFRA), it had good ability to inhibit kinases in the PDK1/PI3K/AKT pathways. Considering VEGFR1/2 and PDGFRA are also really important for tumor growth, **32** may become a good anti-cancer drug instead of a good PDK1 selective inhibitor.

In cell-based systems, **32** and **35** inhibited the phosphorylation of AKT at the Threonine 308 position, which is a direct phosphorylation site for PDK1. Furthermore, the compounds inhibited the downstream activation of the S6 ribosomal protein, which could be an effect of inhibiting PDK1, and also could be the results from the dual inhibition of PDK1 and p70S6K, which functions directly on S6. In a small panel of endometrial cancer cell lines, compounds **32** and **35** demonstrated preferential activity in AN3-CA that was both mutated for PTEN (loss-of-function) and PI3K (gain-of-function), whereas they showed less activity in cell lines that only had a PTEN or PI3K mutation. To test the hypothesis, that **32** and **35** possess preferential activity in cells with both PTEN and PI3K mutations, the breast cancer cell line, HS578T, which has an activating mutation in PI3K and wild type PTEN, was using that treated with PTEN shRNA, to artificially harbor both mutations. In this system, **32** and **35** were 3-fold more potent against the cells with PTEN knockdown compared to the cells that treated with a scrambled shRNA. Although this did not result in a dramatic shift in activity, it supports the idea that these PDK1 inhibitors may be most suitable for development in patients with tumors that harbor mutations in both genes. The absence of a larger shift in activity in these experiments may stem from the fact that the shRNA against PTEN does not completely knockout its expression like a truncating mutation would be in a cancer cell. The knockdown of PTEN as determined by RT-qPCR was approximately 80% after the shRNA treatment.

In order to find out more sensitive cell lines and further prove the hypothesis that has been mentioned in last paragraph, a large cell line panel screen was done with **32** and **35** treatment. The cell lines that turned out to be highly sensitive (KATO3, KG-1, MV4-11, Kasumi-1, MFE296 and AN3-CA) had PTEN deletions or silencing as well as activation of PIK3CA through activating mutations in PIK3CA or ras proteins. Then the whole genome microarray tried to find out any common change that happened in the transcription level among those highly sensitive cell lines. After trying different ways to do the analysis, some common genes were found: DUSP6 and FOSL1 were highly down-regulated, as well as DUSP4, but to a lesser degree. Followed by RT-PCR and Western blot, the changes were confirmed in both the transcription and translation level. With the shRNA experiment, we know that knocking-down these three genes also can kill those sensitive cell lines (AN3-CA, KATO3, MV4-11), but in the varying degrees. The interesting part is, only for MV4-11 cell line, the lethality for knocking-down DUSP6 is almost the same as the drug treatment or knocking-down PDK1. DUSP6 (Dual specificity phosphatase 6) is a protein phosphatase, also known as MKP3. It can dephosphorylate their target kinases in order to inactivate them, so it can negatively regulate members of the MAPK superfamily, which play a role in cellular proliferation and differentiation.[24, 25, 26] As we known it's always hard to cure the cancer by only using one drug, so the combination of DUSP6 inhibitor and PDK1 inhibitor may have a better effect on MV4-11 or biphenotypic B myelomonocytic leukemia.

The developability of these PDK1 compounds[22, 23] as therapeutic agents were further validated by a xenograft model in mice using the AN3-CA cell line, an endometrial cancer cell line that was extremely sensitive to **32** and **35**. In the biochemical and cell-based assays, these two compounds did not differentiate themselves from each other in any meaningful way. However, when dosed at the same level and schedule, **35** was much more active in the *in vivo* xenograft model. Structurally, **32** and **35** differ only be the addition of a methyl group on compound **35**. This improvement *in vivo* activity is likely due to the improved physicochemical properties of **35** over compound **32** with regards to membrane permeability and *in vivo* drug exposure due to metabolism and drug clearance. Therefore, **35,** with its additional methyl group, is likely the more superior of the two compounds to move forward in more advanced animal studies. Pharmacokinetic and more advanced toxicology studies are underway to further explore the possibilities of developing **35** as an anti-

cancer agent. Additionally, **35** has shown to effectively knockdown ribosomal protein S6 signaling in the tumors suggesting the compound has on-target activity.

In conclusion, we have identified compound **35** as a viable PDK1 inhibitor. This compound exhibited good drug-like properties and has demonstrated excellent *in vivo* activity in preliminary animal studies. Compound **35** is currently in more advanced animal studies to characterize pharmacokinetics, pharmacodynamics effects, and limitations due to toxicity. Compound **35** may not be the prefect PDK1 inhibitor, but it has higher possibility to become a novel compound that can be moved forward toward clinical development, particularly in endometrial cancer and others with frequent mutations in both PTEN and PI3K.

Acknowledgments

This work was supported in part by NCI grant P30 CA042014 awarded to the Center for Investigational Therapeutics (CIT) at Huntsman Cancer Institute, as well as funds from the Experimental Therapeutics Program at Huntsman Cancer Institute, University of Utah, 2000 Circle of Hope, Salt Lake City, UT 84112 U.S.A.

References and notes

1. Raimondi, C.; Falasca, M. *Curr. Med. Chem.* **2011**, *18*, 2763-2769.
2. Peifer, C.; Alessi, D. R. *ChemMedChem.* **2008,** *3*, 1810-1838.
3. Chessari, G.; Woodhead, A. J. *Drug Discovery Today*. **2009**, *14*, 668–675.
4. Congreve, M.; Chessari, G.; Tisi, D.; Woodhead, A. J. *J. Med. Chem.* **2008**, *51*, 3661–3680.
5. Friesner, R. A.; Banks, J. L.; Murphy, R. B.; Halgren, T. A.; Klicic, J. J.; Mainz, D. T.; Repasky, M. P.; Knoll, E. H.; Shaw, D. E.; Shelley, M.; Perry, J. K.; Francis, P.; Shenkin, P. S. *J. Med. Chem* **2004**, *47*, 1739–1749.
6. Feldman, R. I.; Wu, J. M.; Polokoff, M. A.; Kochanny, M. J.; Dinter, H.; Zhu, D, Biroc SL, Alicke B, Bryant J, Yuan S, Buckman B.O.; Lentz, D, Ferrer M, Whitlow M, Adler M,Finster S, Chang, Z.; Arnaiz, D. O. *J Biol Chem*. **2005**, *280 (20)*, 9867-9874.
7. McBride, C. M.; Renhowe, P. A.; Heise, C.; Jansen, J. M.; Lapointe, G.; Ma, S.; Piñeda, R.; Vora, J.; Wiesmann, M.; Shafer, C. M. *Bioorg. Med. Chem. Lett*. **2006**, *16*, 3595–3599.
8. Medina, J. R.; Blackledge, C. W.; Heerding, D. A.; Campobasso, N.; Ward, P. B.; Briand, J.; Wright, J.; Axten, J. M. *ACS Med. Chem. Lett*. **2010**, *1*, 439-442.
9. Johnson, M.G.; Hu, Q.; Lingardo, L.; Ferre, R. A.; Greasley, S.; Yan, J.; John, K.; Chen, P.; Jacques, E.; Gordon, A. *J. Computer-Aided Mol. Design* **2011**, *25*, 689-698.
10. **a**) Islam.; I.; Brown, G.; Bryant, J.; Hrvatin, P.; Kochanny, M. J.; Phillips, G. B.; Yuan, S.; Adler, M.; Whitlow, M.; Lentz, D.; Polokoff, M. A.; Wu, J.; Shen, J.; Walters, J.; Ho, E.; Subramanyam, B.; Zhu, D.; Feldman, R. I.; Arnaiz, D. O. *Bioorg. Med. Chem. Lett* **2007**; *17*, 3819-3825, **b**) Islam, I.; Bryant, J.; Chou, Y. L.; Kochanny, M. J.; Lee, W.; Phillips, G. B.; Yu, H.; Adler, M.; Whitlow, M.; Ho, E.; Lentz, D.; Polokoff, M. A.; Subramanyam, B.; Wu, J. M.; Zhu, D.; Feldman, R. I.; Arnaiz, D. O. *Bioorg. Med. Chem. Lett* **2007**, *17*, 3814-3818.
11. Cully, M.; You, H.; Levine, A. J.; Mak, T. W. *Nat Rev Cancer*. **2006**, *6(3)*, 184-192.
12. Angiolini, M.; Banfi, P.; Casale, E.; Casuscelli, F.; Fiorelli, C.; Saccardo, M. B.; Silvagni, M.; Zuccotto, F. *Bioorg. Med. Chem. Lett* **2010**, *20*, 4095–4099.
13. Howard, S.; Berdini, V.; Boulstridge, J. A.; Carr, M. G.; Cross, D. M.; Curry, J.; Devine, L. A.; Early, T. R.; Fazal, L.; Gill. A. L.; Heathcote, M.; Maman, S.; Matthews, J. E.; McMenamin, R. L.; Navarro, E. F.; O'Brien. M. A.; O'Reilly, M.; Rees, D. C.; Reule, M.; Tisi, D.; William, G.; Vinković, M.; Wyatt, P.G. *J. Med. Chem* **2009**, *52*, 379-388.
14. Xu, Z.; Nagashima, K.; Sun, D.; Rush, T.; Northrup, A.; Andersen, J. N.; Kariv, I.; Bobkova, E. V. *J. Biomol. Screen* **2009**, *14*, 1257-1262.
15. Suite 2011**,** QikProp, version 3.4, Schrödinger, LLC, New York, NY, 2011.
16. Calculator Plugins Calculator Plugins were used for structure property prediction and calculation, Marvin Sketch (6.1.2), 201n (2013), ChemAxon (http://www.chemaxon.com).
17. Early, T. R.; Fazal, L.; Gill. A. L.; Heathcote, M.; Maman, S.; Matthews, J. E.; McMenamin, R. L.; Navarro, E. F.; O'Brien. M. A.; O'Reilly, M.; Rees, D. C.; Reule, M.; Tisi, D.; William, G.; Vinković, M.; Wyatt, P.G. *J. Med. Chem* **2009**, *52*, 379-388.
18. Abagyan, R.; Totrov, M.; Kuznetsov, D. *J. Comput. Chem* **1994**, *15*, 488-506.
19. Poulsen, A.; Blanchard, S.; Soh, C. K.; Lee, C.; Williams, M.; Wang, H.; Dymock, B. *Bioorg. Med. Chem. Lett* **2012**, *22*, 305-307.
20. Humphrey, J.; Kablaoui, N.; Kazmirski, S.; Kraus, M.; Kupchinsky, S.; Li. J.; Lingardo, L.; Marx, M. A.; Richter. D.; Tanis, S. P.; Tran, K.; Vernier, W.; Xie, Z.; Yin, M. J.; Yu, X. H. *J. Med. Chem* **2011**, *54*, 8490-8500.
21. Medina, J. R.; Becker, C. J.; Blackledge, C. W.; Duquenne, C.; Feng, Y. Grant, S. W.; Heerding, D.; Li, W. H.; Miller, W. H.; Romeril, S. P.; Scherzer, D.; Shu, A.; Bobko, M. A.; Chadderton, A. R.; Dumble, M.; Gardiner, C. M.; Gilbert, S.; Liu, Q.; Rabindran, S. K.; Sudakin, V.; Xiang, H.; Brady, P. G.; Campobasso, N.; Ward, P.; Axten, J. M. *J. Med. Chem* **2011**, *54*, 1871-195.
22. Najafov, A.; Sommer, E. M.; Axten, J. M.; Deyoung, M. P.; Alessi, D. R.; Dario, R. *Biochem J* **2011**, 433, 357-369.
23. Bearss, D. J.; Vankayalapati, H.; Sorna, V.; Warner, S, L.; Sharma, S. PCT Int. WO 2012135799 A1. Appl 2012.
24. Patterson K.I.; Brummer T.; O'Brien P.M.; Daly R.J.. *Biochem. J.* **2009**, *418*, 475–489.
25. Caunt C.J.; Keyse S.M.. *FEBS J*. **2013**, *280*, 489–504
26. Bermudez O.; Pagès G.; Gimond C.. *Am. J. Physiology - Cell Physiology*. **2010**, *299*, C189–C202

Supplementary Material

Supplementary data (experimental information details and supporting tables and figures) associated with this article can be found, in the online version.

[±]Current Address:
TGen, 445 N. 5th Street, Phoenix, AZ 85004, USA.
Email: hvankayalapati@tgen.org

Table 1. Inhibition of PDK1 by 1*H*-benzo[*d*]imidazol-2-yl)-1*H*-indazol derivatives.

Compound	Structure	[a] IC_{50} µM	Compound	Structure	[a] IC_{50} µM
19	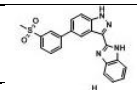	15.3	**20**	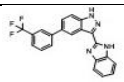	30.3
21	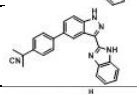	5.2	**22**	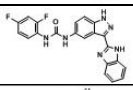	[b]NA
23	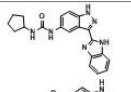	53.9	**24**	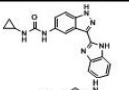	0.9
25	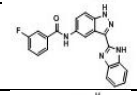	8.8	**26**	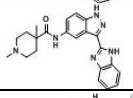	12.4
27	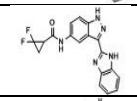	0.3	**28**	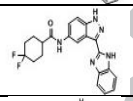	0.4
29	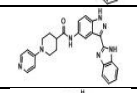	[b]NA	**30**	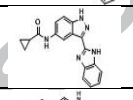	1.2
31	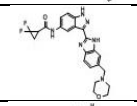	1.2	**32**	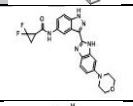	0.08
33	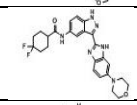	0.2	**34**	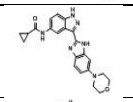	0.2
35	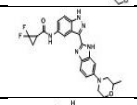	0.09	**36**	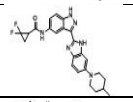	0.8
37	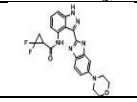	0.4	**38**	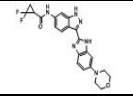	[b]NA

Graphical Abstract

Fragment-Based Design, Synthesis, Biological Evaluation, and SAR of 1H-benzo[*d*]imidazol-2-yl)-1H-indazol Derivatives as Potent PDK1 Inhibitors

Ting Chen, Venkataswamy Sorna, Susie Choi, Lee Call, Jared Bearss, Kent Carpenter, Steven L. Warner, Sunil Sharma, David J. Bearss, Hariprasad Vankayalapati